Supplemental Data

The Vacuolar H^+-ATPase Mediates Intracellular Acidification Required for Neurodegeneration in *C. elegans*

Popi Syntichaki, Chrysanthi Samara, and Nektarios Tavernarakis

Supplemental Experimental Procedures

Strains and Genetics

We followed standard procedures for *C. elegans* strain maintenance, crosses, and other genetic manipulations [S1].The nematode rearing temperature was kept at 20°C, unless otherwise noted. The following strains were used in this study: wild-type N2 Bristol isolate, *deg-3(u662)V*, referred to in the text as *deg-3(d)*; *mec-4(u231)X*, referred to in the text as *mec-4(d)*; and *spe-5(hc93)I;sDp2(I;f)*, *unc-32(e189)III*, *vha-12(n2915)X*, and *nuIs5*[$p_{glr\text{-}1}G\alpha_s$(Q227L) $p_{glr\text{-}1}$GFP], referred to in the text as α_s*(gf)* [S2]. The following double and multiple mutants were examined for neurodegeneration: *spe-5(hc93)I; mec-4(u231)X*, *unc-32(e189)III;deg-3(u662)V*, *unc-32(e189)III;mec-4(u231)X*, *unc-32(e189)III;nuIs5*[$p_{glr\text{-}1}G\alpha_s$(Q227L)$p_{glr\text{-}1}$GFP], *deg-3(u662)V; vha-12(n2915)X*, *vha-12(n2915)mec-4(u231)X*, and *vha-12(n2915)X; nuIs5*[$p_{glr\text{-}1}G\alpha_s$(Q227L)$p_{glr\text{-}1}$GFP]. *spe-5(hc93)I* mutant animals are sterile as a result of a spermatogenesis defect [S3]. We constructed the *spe-5(hc93)I;mec-4(u231)X* double mutant by crossing fertile *spe-5(hc93)I;sDp2(I;f)* hermaphrodites carrying the wild-type *spe-5* gene on the free chromosome I duplication *sDp2(I;f)* with *mec-4(u231)X* males. The presence of *sDp2(I;f)* complements the spermatogenesis defect in *spe-5(hc93)I* mutants. *sDp2(I;f)* is unstable during mitosis and is lost in about 70% of *spe-5(hc93)I;sDp2(I;f)* progeny. Cell death was suppressed only in those double-mutant individuals not carrying the free duplication.

Plasmid Constructs and RNA Iinterference

pHluorin reporter constructs were generated by fusion of the touch-receptor-neuron-specific *mec-7* promoter to ratiometric pHluorin GFP (RmpHluorin) [S4] or superecliptic pHluorin GFP (SepHluorin) [S5]. A BamHI-EcoRI fragment containing the coding region of the ratiometric or the ecliptic pHluorin was amplified from the original constructs in the pGEX-2T vector [S4]. Similarly, a BamHI-EcoRI fragment containing the coding region of the super-ecliptic pHluorin was amplified from the original pGEX-4T2 vector [S5]. In all cases the set of primers used for the amplification was 5′-CCGCTCGA GATGGGATCCACCGGTGGAAG-3′ and 5′-GAAGATCTCTAGAATT CACCGGTTTTG-3′. The resulting 761 bp PCR products were cloned into the pPD96.41 plasmid vector downstream of the *mec-7* promoter [S6]. Together with plasmid pRF4 carrying the dominant transformation marker *rol-6(su1006)*, these plasmids were each injected into the gonads of N2 animals. We crossed transgenic, roller hermaphrodites with *mec-4(d)* and *vha-12(n2915)mec-4(d)* males to generate mutants carrying pHluorin reporter constructs.

For RNAi experiments, we constructed plasmids that direct the synthesis of dsRNAs corresponding to *vha-2*, *vha-10*, and *vha-12*. We used *E. coli* bacteria, which were fed to animals according to a previously described methodology [S7]. RNAi plasmids for aspartyl proteases *asp-3* and *asp-4* and calpain *clp-1* have been described previously [S8]. For *vha-10*, we cloned an 889 bp BamHI-HindIII PCR fragment that corresponds to the *vha-10* coding region into the pL4440 plasmid vector [S9] by using the primers described previously [S10]. For *vha-2*, we cloned a 476 bp BamHI-HindIII PCR fragment derived from the *vha-2* locus into the pL4440 plasmid vector [S9] by using the primers described previously [S11]. For *vha-12*, we amplified a 1.43 Kb XbaI-HindIII PCR fragment containing the *vha-12* coding sequence and cloned it into the pL4440 plasmid vector [S9] by using the primers 5′-GCTCTAGAATGGCTGCCGTT GACGTC-3′ and 5′-CCCAAGCTTGGGTGATGAAGTTCTTC-3′. We used RNAi in addition to antibiotic inhibitors and mutations in specific subunits to incapacitate the V-ATPase in *mec-4(d)*, *deg-3(d)*, and α_s*(gf)* genetic backgrounds. As a positive control in these experiments, we knocked down *crt-1*, which encodes calreticulin, an endoplasmic reticulum chaperone known to be required for *mec-4(d)*- and α_s*(gf)*- but not *deg-3(d)*-induced neurodegeneration [S12]. RNAi with *gfp* was used as a negative control. Although RNAi is relatively ineffective for genes expressed in mature *C. elegans* neurons (N.T. and P.S., unpublished data) [S13], we observed suppression of neurodegeneration triggered by *mec-4(d)* both in *crt-1(RNAi)* animals

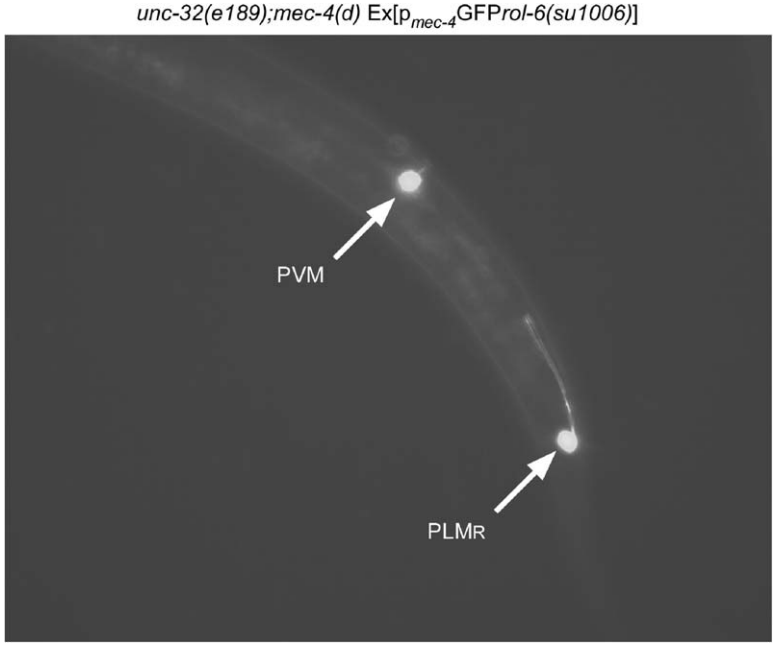

Figure S1. Surviving Touch Cells in an *unc-32(e189);mec-4(d)* Double Mutant

Neurons express a $p_{mec\text{-}4}$GFP reporter. Less than 1% of *mec-4(d)* animals carrying the $p_{mec\text{-}4}$GFP transgene show fluorescent PLM neurons at adulthood. About 15% of *unc-32(e189);mec-4(d)* double-mutant adults show fluorescent touch receptors ($n = 200$, $p < 0.001$, unpaired t test).

Table S1. *C. elegans* Vacuolar H^+-ATPase Genes

Gene	ORF	Chromosome	Subunit/Domain[a]	Yeast Protein	Expression[b]	Mutant/RNAi Phenotype	Reference
vha-1	R10E11.8	III	17 kDa proteolipid c subunit, V0 domain	Vma11p/Tfp3p	excretory canal cell, rectum, two post-anal cells	embryonic lethal	[S19, S25]
vha-2	R10E11.2	III	16.4 kDa proteolipid c subunit, V0 domain	Vma11p/Tfp3p	excretory canal cell, rectum, two post-anal cells	embryonic lethal	[S19, S26, S27]
vha-3	Y38F2AL.4	IV	16.4 kDa proteolipid c subunit, V0 domain	Vma11p/Tfp3p	excretory canal cell, gastrointestinal cells, hypodermal cells	embryonic lethal	[S20, S26]
vha-4	T01H3.1	II	22.1 kDa proteolipid c'' subunit, V0 domain	Ppa1p	excretory canal cell, rectum, a pair of cells near the anus	embryonic lethal	[S19, S23, S26]
vha-5	F35H10.4	IV	99.3 kDa a subunit, V0 domain	Vph1p/Stv1p	excretory canal cell, pharynx, hypodermal cells around the vulva	larval lethal	[S21, S22, S26]
vha-6	VW02B12L.1	II	98.5 kDa a subunit, V0 domain	Vph1p/Stv1p	intestine	larval lethal	[S21, S22, S26]
vha-7	C26H9A.1	IV	110.5 kDa a subunit, V0 domain	Vph1p/Stv1p	hypodermal cells, uterus, early oocytes, spermateca	wild-type	[S21, S22, S28]
vha-8	C17H12.14	IV	25.6 kDa E subunit, V1 domain	Vma4p	excretory canal cell, lateral hypodermis	embryonic lethal	[S29, S30]
vha-9	ZK970.4	II	13.3-kDa F subunit, V1 domain	Vma7p	—	embryonic lethal	[S26]
vha-10	F46F11.5	I	14.5-kDa G subunit, V1 domain	Vma10p	excretory canal cell, nerve-ring neurons, ventral nerve-cord motorneurons, body-wall muscles, vulva muscles, intestine	embryonic lethal	[S10], this study
vha-11	Y38F2AL.3	IV	43.5 kDa C subunit, V1 domain	Vma5p	excretory canal cell, intestine	embryonic lethal, Sterile	[S11, S20, S26]
vha-12	F20B6.2	X	54.8 kDa B subunit, V1 domain	Vma2p	—	embryonic lethal, uncoordinated (allele n2915)	[S25, S26], R. Weimer and E. Jorgensen, University of Utah, personal communication
vha-13	Y49A3A.2	V	44.3 kDa A subunit, V1 domain	Vma1p	—	embryonic lethal	[S25, S26]
vha-14	F55H2.2	III	28.8 kDa D subunit, V1 domain	Vma8p	—	embryonic lethal	[S27]
vha-15	T14F9.1	X	54.2 kDa H subunit, V1 domain	Vma13p	—	embryonic lethal	[S25, S28]
vha-16	C30F8.2	I	39.9 kDa d subunit, V0 domain	Vma6p	—	—	—
vha-17	F49C12.13	IV	10.9 kDa e subunit, V0 domain	Vma9p-		embryonic lethal	[S24–S26]
spe-5	Y110A7A.12	I	56 kDa B subunit, V1 domain	Vma2p	—	spermatogenesis defective	[S3], P.D. Hartley, G.-d. Zhu, and S.W. L' Hernault, Emory University, personal communication
unc-32	ZK637.8	III	103.4 kDa a subunit, V0 domain	Vph1p/Stv1p	intestine, gonad, nerve-ring neurons, ventral-nerve-cord motorneurons	embryonic lethal, Reverse ventral coiler (allele e189)	[S21, S22, S25–S27]

The *vha-8* gene is also known as *pes-6* (WormBase release WS123; http://www.wormbase.org/). Elimination of most genes encoding V-ATPase subunits by mutation or RNAi results in severe embryonic lethality or sterility, highlighting the essential function of this pump. The most severe phenotype associated with genome-wide RNAi studies reported in the literature and in WormBase is noted.

[a] Estimated size of predicted *C. elegans* proteins.

[b] Not readily detectable; low-level expression in additional cells cannot be ruled out.

and in animals subjected to RNAi with various V-ATPase subunits (Figures 1A and 1C in the main text) [S8]. Probably, RNAi is more effective with genes expressed at early developmental stages in the nervous system (degeneration occurs soon after the touch-receptor neurons are born during late embryogenesis and the first larval stage in *mec-4(d) C. elegans* mutants) [S14]. We assayed the effectiveness of RNAi with V-ATPase gene expression by monitoring the expression of full-length *vha-n*::GFP reporter fusions.

Neurodegeneration Assays

Degeneration of specific neuron sets in animals bearing *deg-3(d)*, *mec-4(d)*, and α_s*(gf)* alleles was quantified as described previously [S8]. To simulate death-inducing, hypoxic conditions, we treated nematodes at the L4 stage of development with sodium azide (NaN_3; 0.5 M, 30 min at 20°C; Sigma, Munich, Germany; adapted with modifications from [S15]). V-ATPase inhibitors (50 μM bafilomycin A1, LC Laboratories, Woburn, Massachusetts; 30 μM filomycin, Sigma, Munich, Germany) were administered by injection in the body cavity of gravid adults, and neurodegeneration was assayed in the progeny of injected individuals. Thapsigargin-induced cell death was assayed as described previously (animals were treated with 10 μg/ml thapsigargin; Sigma, Munich, Germany) [S12]. Statistical analysis of data was carried out with the Microsoft Office 2003 Excel software package (Microsoft Corporation, Redmond, Washington).

In *mec-4(d)* animals, the ALM and PLM neurons suffer death more frequently than the AVM and PVM neurons do [S8, S12, S16]. Although all six touch receptors are at the threshold of degeneration, ALMs and PLMs are more likely to die because they express the *mec-4* gene at higher levels (our unpublished observations) [S14]. Any single *mec-4(d)* L1 animal may show from zero to six degenerating cells. Similar effects are observed in *deg-3(d)* and α_s*(gf)* genetic backgrounds. Because of the stochastic nature of neurodegeneration, large numbers of individuals are routinely analyzed in order to infer significance (at least 200 individuals in typically three independent experiments, with a p value of less than 0.001, unpaired t test). When degeneration is suppressed, the surviving neurons still express the mutant *mec-4(d)*. Therefore, these neurons do not function as touch receptors because MEC-4, one of the core subunits of the presumed mechanosensory channel, is incapacitated. This is generally the case with extragenic necrosis suppressors that intercept necrosis at downstream nodes of the cell-death pathway (i.e., *mec-6*, calreticulin, calpains, and cathepsins; see for example [S12]. Nevertheless, these neurons express various GFP reporter fusions, differentiate, and fasciculate normally (Figure S1). In cases in which the toxic *mec-4(d)* allele is expressed ectopically in other neurons that do not require MEC-4, their function is fully restored when neurodegeneration is suppressed (for example, upon ectopic expression of *mec-4(d)* in motorneurons) [S12, S17]. Interestingly, in double mutants and in RNAi experiments, where neurodegeneration is significantly suppressed, not only is the number of vacuoles lower, but incident vacuoles are also qualitatively different; they are smaller and less pronounced than in *mec-4(d)* single mutants.

Intracellular pH Monitoring

We adapted the methods described previously ([S4]; [S5]) to visualize pH changes in dying *C. elegans* touch-receptor neurons. Synchronized cultures of transgenic N2, *mec-4(d)*, and *vha-12(n2915)mec-4(d)* nematodes carrying superecliptic or ratiometric pHluorin were harvested at the L1 stage of development. Animals were scanned with a 476 nm laser beam under a confocal microscope. Images of emission from individual PLM touch-receptor neurons were acquired with a 515 ± 15 nm band-pass filter. These neurons are embedded in the hypodermis and are not readily accessible to pH-buffering solutions. To assess intracellular pH changes during necrosis, we measured differences in pHluorin emission intensity (ΔF) between wild-type and degenerating neurons on grayscale images with a color depth of 8 bit (256 shades of gray). For each neuron, we accumulated a Z stack of flat xy images spanning its entire depth and produced the maximum projection of these images across the whole cell area. We calculated the mean and maximum pixel intensity in these projections by using the ImageJ software (http://rsb.info.nih.gov/ij/). For each transgenic line, we processed at least 150 neuron images over three independent trials. Statistical analysis was carried out with the Microsoft Office 2003 Excel software package.

Bioinformatics

The GenBank accession numbers for VHA-10 and the Vacuolar H^+-ATPase G-subunit sequences used for the analysis are as follows: *Caenorhabditis elegans* VHA-10, NP_491641.1; *Caenorhabditis briggsae* VHA-10, CAE68925; *Saccharomyces cerevisiae* Vma10p, NP_011905.1; *Manduca sexta* vacuolar H^+-ATPase G subunit, Q25532; *Drosophila melanogaster* vacuolar H^+-ATPase G subunit, NP_477437.1; *Homo sapiens* vacuolar H^+-ATPase G subunit, NP_004879.1. BLAST searches ([S18]) were performed with the National Center for Biotechnology Information web servers (NCBI; http://www.ncbi.nlm.nih.gov/BLAST/).

The *C. elegans* V-ATPase

Seventeen of the 19 genes that encode the 13 V-ATPase subunits in *C. elegans* bear the generic name *vha* (vacuolar H^+-ATPase; Table S1). Most subunits of the yeast V-ATPase share extensive similarity with several predicted *C. elegans* proteins. For each, we note the best match, identified by BLAST search in Table S1. Genes that correspond to multiple isoforms for each V-ATPase subunit show different spatiotemporal expression and may have tissue- or development-specific roles in addition to encoding redundant functions [S11, S19–S22]. For our analysis, we chose to target V-ATPase genes showing discernible expression in the nervous system, including the neurons subjected to degeneration, with expression timing overlapping with that of cell death (*vha-2*, *vha-10*, *vha-12*), and ones with available mutant alleles (*spe-5*, *unc-32*, *vha-12*). V-ATPase subunits are organized into a macromolecular complex composed of two discrete domains. The peripheral V1 domain, with a size approximating 640 kDa, is assembled from eight different subunits (A–H) and is responsible for ATP hydrolysis. The V0 domain, with a size of about 260 kDa, is the membrane-integral part that carries out proton translocation and is composed of six different subunits (a, d, e, c, c′, c″) [S23, S24]. Apart from proton translocation across membranes, the V0 sector of the V-ATPase has been specifically implicated in membrane fusion events (reviewed by [S23]). Targeting genes encoding subunits of both the V0 and V1 peripheral sector suppressed necrosis. Additionally, the antibiotics bafilomycin A1 and filomycin, whcih inhibit the V-ATPase pump, ameliorated cell death. Thus, we consider a specific requirement for the V0 sector membrane-fusion function in necrosis unlikely.

Complete loss-of-function mutations or strong RNAi in essential V-ATPase subunits result in embryonic lethality, developmental arrest, or sterility (Table S1). Similar detrimental effects are observed after prolonged treatment with V-ATPase inhibitors such as the antibiotics bafilomycin and filomycin. By controlling for exposure to dsRNA in *C. elegans*, one can induce an array of phenotypes that range in severity. In our experiments, conditions were such that they would allow for normal development of progeny past the L1 stage, where we assay for cell death. Also, combinatorial RNAi with more than one *vha* gene, or RNAi on top of *vha* mutant alleles, produced more-severe synthetic phenotypes, to the point of complete sterility, which did not allow assay of cell-death suppression. Generally, in these experiments suppression correlated with the severity of embryonic lethality. Controlled treatment with both bafilomycin and filomycin recapitulated these effects.

Supplemental References

S1. Brenner, S. (1974). The genetics of Caenorhabditis elegans. Genetics *77*, 71–94.

S2. Berger, A.J., Hart, A.C., and Kaplan, J.M. (1998). G alpha-induced neurodegeneration in Caenorhabditis elegans. J. Neurosci. *18*, 2871–2880.

S3. Machaca, K., and L'Hernault, S.W. (1997). The Caenorhabditis elegans spe-5 gene is required for morphogenesis of a sperm-specific organelle and is associated with an inherent cold-sensitive phenotype. Genetics *146*, 567–581.

S4. Miesenbock, G., De Angelis, D.A., and Rothman, J.E. (1998).

Visualizing secretion and synaptic transmission with pH-sensitive green fluorescent proteins. Nature *394*, 192–195.

S5. Sankaranarayanan, S., De Angelis, D., Rothman, J.E., and Ryan, T.A. (2000). The use of pHluorins for optical measurements of presynaptic activity. Biophys. J. *79*, 2199–2208.

S6. Fire, A., Harrison, S.W., and Dixon, D. (1990). A modular set of lacZ fusion vectors for studying gene expression in Caenorhabditis elegans. Gene *93*, 189–198.

S7. Kamath, R.S., Martinez-Campos, M., Zipperlen, P., Fraser, A.G., and Ahringer, J. (2001). Effectiveness of specific RNA-mediated interference through ingested double-stranded RNA in Caenorhabditis elegans. Genome Biol *2*, RESEARCH0002.

S8. Syntichaki, P., Xu, K., Driscoll, M., and Tavernarakis, N. (2002). Specific aspartyl and calpain proteases are required for neurodegeneration in C. elegans. Nature *419*, 939–944.

S9. Timmons, L., Court, D.L., and Fire, A. (2001). Ingestion of bacterially expressed dsRNAs can produce specific and potent genetic interference in Caenorhabditis elegans. Gene *263*, 103–112.

S10. Fraser, A.G., Kamath, R.S., Zipperlen, P., Martinez-Campos, M., Sohrmann, M., and Ahringer, J. (2000). Functional genomic analysis of C. elegans chromosome I by systematic RNA interference. Nature *408*, 325–330.

S11. Oka, T., and Futai, M. (2000). Requirement of V-ATPase for ovulation and embryogenesis in Caenorhabditis elegans. J. Biol. Chem. *275*, 29556–29561.

S12. Xu, K., Tavernarakis, N., and Driscoll, M. (2001). Necrotic cell death in *C. elegans* requires the function of calreticulin and regulators of Ca(2+) release from the endoplasmic reticulum. Neuron *31*, 957–971.

S13. Tavernarakis, N., Wang, S.L., Dorovkov, M., Ryazanov, A., and Driscoll, M. (2000). Heritable and inducible genetic interference by double-stranded RNA encoded by transgenes. Nat. Genet. *24*, 180–183.

S14. Hall, D.H., Gu, G., Garcia-Anoveros, J., Gong, L., Chalfie, M., and Driscoll, M. (1997). Neuropathology of degenerative cell death in Caenorhabditis elegans. J. Neurosci. *17*, 1033–1045.

S15. Scott, B.A., Avidan, M.S., and Crowder, C.M. (2002). Regulation of hypoxic death in C. elegans by the insulin/IGF receptor homolog DAF-2. Science *296*, 2388–2391.

S16. Driscoll, M., and Chalfie, M. (1991). The mec-4 gene is a member of a family of Caenorhabditis elegans genes that can mutate to induce neuronal degeneration. Nature *349*, 588–593.

S17. Tavernarakis, N., Shreffler, W., Wang, S., and Driscoll, M. (1997). unc-8, a DEG/ENaC family member, encodes a subunit of a candidate mechanically gated channel that modulates *C. elegans* locomotion. Neuron *18*, 107–119.

S18. Altschul, S.F., Madden, T.L., Schaffer, A.A., Zhang, J., Zhang, Z., Miller, W., and Lipman, D.J. (1997). Gapped BLAST and PSI-BLAST: a new generation of protein database search programs. Nucleic Acids Res. *25*, 3389–3402.

S19. Oka, T., Yamamoto, R., and Futai, M. (1997). Three vha genes encode proteolipids of Caenorhabditis elegans vacuolar-type ATPase. Gene structures and preferential expression in an H-shaped excretory cell and rectal cells. J. Biol. Chem. *272*, 24387–24392.

S20. Oka, T., Yamamoto, R., and Futai, M. (1998). Multiple genes for vacuolar-type ATPase proteolipids in Caenorhabditis elegans. A new gene, vha-3, has a distinct cell-specific distribution. J. Biol. Chem. *273*, 22570–22576.

S21. Oka, T., Toyomura, T., Honjo, K., Wada, Y., and Futai, M. (2001). Four subunit a isoforms of Caenorhabditis elegans vacuolar H+-ATPase. Cell-specific expression during development. J. Biol. Chem. *276*, 33079–33085.

S22. Pujol, N., Bonnerot, C., Ewbank, J.J., Kohara, Y., and Thierry-Mieg, D. (2001). The Caenorhabditis elegans unc-32 gene encodes alternative forms of a vacuolar ATPase a subunit. J. Biol. Chem. *276*, 11913–11921.

S23. Nishi, T., and Forgac, M. (2002). The vacuolar (H+)-ATPases—nature's most versatile proton pumps. Nat. Rev. Mol. Cell Biol. *3*, 94–103.

S24. Merzendorfer, H., Huss, M., Schmid, R., Harvey, W.R., and Wieczorek, H. (1999). A novel insect V-ATPase subunit M9.7 is glycosylated extensively. J. Biol. Chem. *274*, 17372–17378.

S25. Kamath, R.S., Fraser, A.G., Dong, Y., Poulin, G., Durbin, R., Gotta, M., Kanapin, A., Le Bot, N., Moreno, S., Sohrmann, M., et al. (2003). Systematic functional analysis of the Caenorhabditis elegans genome using RNAi. Nature *421*, 231–237.

S26. Simmer, F., Moorman, C., Van Der Linden, A.M., Kuijk, E., Van Den Berghe, P.V., Kamath, R., Fraser, A.G., Ahringer, J., and Plasterk, R.H. (2003). Genome-wide RNAi of C. elegans using the hypersensitive rrf-3 strain reveals novel gene functions. PLoS Biol. 1, e12. 10.1371/journal.pbio.0000012.

S27. Gonczy, P., Echeverri, C., Oegema, K., Coulson, A., Jones, S.J., Copley, R.R., Duperon, J., Oegema, J., Brehm, M., Cassin, E., et al. (2000). Functional genomic analysis of cell division in C. elegans using RNAi of genes on chromosome III. Nature *408*, 331–336.

S28. Maeda, I., Kohara, Y., Yamamoto, M., and Sugimoto, A. (2001). Large-scale analysis of gene function in Caenorhabditis elegans by high-throughput RNAi. Curr. Biol. *11*, 171–176.

S29. Choi, K.Y., Ji, Y.J., Dhakal, B.K., Yu, J.R., Cho, C., Song, W.K., and Ahnn, J. (2003). Vacuolar-type H+-ATPase E subunit is required for embryogenesis and yolk transfer in Caenorhabditis elegans. Gene *311*, 13–23.

S30. Hope, I.A., Albertson, D.G., Martinelli, S.D., Lynch, A.S., Sonnhammer, E., and Durbin, R. (1996). The C. elegans expression pattern database: A beginning. Trends Genet. *12*, 370–371.